TEKNIKA: JURNAL SAINS DAN TEKNOLOGI

Homepage journal: http://jurnal.untirta.ac.id/index.php/ju-tek/

Original research article

Thermal effectiveness comparison analysis on air-based PV/T system with varying top-to-bottom cavity ratios using CFD simulation

Nabil Putra Wahyu Yanuariska [a,*], Nia Nuraeni Suryaman [a], Ahmad Rajani [b]

[a] *Department of Mechanical Engineering, Widyatama University, Bandung, 40126, Indonesia*

[b] *Research Centre for Energy Conversion and Conservation, BRIN, Indonesia*

ARTICLE INFO

Article history
Submitted 15 May 2025
Received in revised form 12 June 2025
Accepted 22 June 2025
Available online 24 June 2025

Keywords
Photovoltaic Thermal (PV/T)
CFD simulation
Turbulence intensity
Effective thermal conductivity
Outlet temperature

Editor:
Dwinanto

Publisher's note:
The publisher remains neutral regarding jurisdictional claims in published maps and institutional affiliations, while the author(s) bear sole responsibility for the accuracy of content and any legal implications.

ABSTRACT

The development of air-based thermal photovoltaic systems is still challenged in optimizing heat transfer efficiency. One important aspect in this endeavor is to find and improve the cooling channel geometry design. To address this, this study aims to evaluate the effect of several variations of upper and lower cavities on the performance of dual-pass PV/T systems using a computational fluid dynamics (CFD) simulation approach. Four geometry ratio configurations (1:1, 1:4, 2:3, and 3:2) were analyzed based on turbulence intensity, effective thermal conductivity, and air temperature output. The investigation results show that the 3:2 configuration excels in several parameters. The findings highlighted that the 3:2 geometry showed improved turbulence generation and heat exchanger efficiency compared to the other shapes. Specifically, the 3:2 geometry generated turbulence intensity reaching 78% compared to the other geometries, which did not even reach 60%. In addition, the 3:2 geometry produces superior effective thermal conductivity and the most uniform heat transfer. Meanwhile, the 1:4 configuration achieved the highest outlet temperature of 29.54°C, making this geometry potentially suitable for solar energy-based drying applications. The investigation results provide practical insights and geometry-based PV/T system design alloys to improve energy efficiency in sustainable thermal applications.

1. Introduction

The emergence of renewable energy, particularly solar energy, offers a solution to global challenges such as climate change, dependence on fossil fuels, and increasing energy demand driven by global population growth [1]. Energy plays a critical role in economic development and improving people's well-being, as evidenced by historical data linking energy availability to sustainable economic activity [2]. However, the continued use of fossil fuels has significant environmental impacts, including increased greenhouse gas emissions and global warming, which are

* Corresponding author
Email address: nabil.wahyu@widyatama.ac.id

DOI: http://dx.doi.org/10.62870/tjst.v21i1.32679

major contributors to climate change [3]. In this context, solar energy, as a primary source of heat and light, serves as a sustainable alternative. Its environmentally friendly utilization significantly reduces reliance on harmful fossil fuels while supporting the transition to sustainable energy systems [4].

Over the past few decades, the solar-based power generation market, utilizing thermal and photovoltaic (PV) technologies, has grown rapidly [5, 6]. One approach to improving the effectiveness of these systems involves reducing heat in the collector to enhance PV performance [7]. To address heat-related issues, incorporating air collectors in hybrid photovoltaic-thermal (PV/T) systems is a potential solution [8]. Hybrid PV/T collector technology is a viable option under certain conditions, as it can reduce costs by producing both electrical and thermal energy simultaneously [9]. This system uses fluid—either air or water—to absorb heat while generating electrical and thermal energy. Modifications to airflow, through either free or forced convection, and cooling system designs with fluids directly connected to PV modules can enhance overall efficiency [10]. By utilizing the heat generated by PV modules as a thermal energy source, PV/T systems not only prevent excessive temperature rises in the modules, which can reduce electrical efficiency, but also offer ease of implementation and maintenance, particularly in air-based systems [11].

Various studies have examined the efficiency and characteristics of PV/T systems through laboratory-scale simulations and real-world testing. Patil et al. presented a CFD analysis of PV/T systems with active bottom air cooling to enhance performance [12]. Yang et al. compared PV/T-PCM systems with conventional PV/T systems, finding that phase change materials (PCM) improve efficiency by managing PV module temperatures and extending energy service time for targeted buildings [13]. Prasetyo et al. compared various PV/T system designs, including collector configurations, the use of fins in collectors, and flow modeling in finned collectors [14]. Rajani et al. analyzed the efficiency of turn-shape geometry at the rear of PV/T systems, noting that the triangular bend geometry exhibited the highest turbulence intensity of approximately 70%, compared to other shapes at around 60%, along with more effective heat exchange [15].

The development of photovoltaic-thermal (PV/T) systems continues to focus on achieving optimal energy efficiency through experiments with collector designs that maximize electrical and thermal energy conversion. Air-based PV/T collectors have been repeatedly tested and proven effective in increasing both thermal and electrical efficiency [16]. The most commonly used configurations are single-pass and double-pass systems. In a single-pass system, the coolant flows through the collector once, resulting in shorter contact time between the fluid and the collector, which may reduce heat transfer efficiency. In contrast, a double-pass system allows the fluid to flow through two channels, increasing contact time with the collector surface and potentially improving thermal efficiency, especially in areas with high solar radiation intensity. Research by Amrizal et al. showed that air-based PV/T collectors with dual-pass paths can achieve a thermal efficiency of 73.23% and an electrical efficiency of 10.16% at a fluid mass flow rate of 0.048 kg/s [17]. Additionally, air-cooled collectors are cost-effective due to their simpler design.

However, water-based PV/T collectors also offer superior heat absorption capacity, as water has a higher heat capacity than air. These collectors are effective in managing PV module temperatures and maintaining overall system efficiency, particularly in applications requiring stable temperature control, such as water heating and industrial processes [18, 19]. Kazem reported that water-based PV/T systems produce more consistent and stable thermal energy, although challenges include the complexity of fluid circulation systems and higher installation costs [18]. This aligns with research by Barone et al., which found that more efficient fluid circulation systems in water-based PV/T collectors can significantly improve heat transfer, potentially increasing overall system efficiency [20]. Additionally, the development of bifacial solar panel technology has emerged as an effective innovation for improving PV/T efficiency [21]. Bifacial panels capture sunlight from both the front and back sides of the module, increasing electricity generation by utilizing reflected sunlight from the ground or other surfaces [22, 23]. In combination with air-based PV/T systems, bifacial panels can provide additional benefits, enhancing both electrical and thermal energy production. Research by Kurz et al. demonstrated that bifacial panels can increase electricity production by more than 56% compared to monofacial panels, offering significant advantages for photovoltaic installation design [24]. Furthermore, Tina and Gagliano confirmed that integrating bifacial panels into PV/T systems can significantly improve both thermal and electrical efficiency, potentially reducing long-term operational costs [25].

Overall, the combination of bifacial panel technology, air-based PV/T collectors, and double-pass systems offers a more efficient and sustainable solution for harnessing solar energy [26]. The selection of the upper-to-lower cavity ratio as a primary variable is based on its significant influence on airflow distribution and heat transfer within air-based PV/T systems. Variations in cavity geometry can lead to different thermal efficiencies by optimizing the contact area between the working fluid and the heat-absorbing surface. Rajani et al. reported that asymmetry in the upper cavity channel and lower cavity can increase thermal efficiency by up to 8% [27]. However, studies examining the influence of this cavity ratio using CFD approaches remain limited. With optimized collector designs, more efficient materials, and a deeper understanding of the interactions between these elements, PV/T systems are expected to evolve into a more energy-efficient and environmentally friendly renewable energy solution [28].

Although several studies have explored PV/T systems, specific research on the effect of upper-to-lower cavity ratio variations using CFD simulations in air-based systems remains scarce. Therefore, this study aims to fill this gap by exploring the thermal performance and efficiency of photovoltaic-thermal (PV/T) systems with various geometric design variations, particularly focusing on the upper and lower cavity ratios. Using a computational fluid dynamics (CFD)-based simulation approach, this study seeks to identify the optimal configuration to enhance fluid flow and heat transfer in PV/T collectors. The primary goal is to provide deeper insights into the effects of design modifications on temperature distribution and thermal performance, thereby improving the overall efficiency of PV/T systems. The results of this study are expected to contribute to the development of more efficient and practical PV/T systems and support innovations in sustainable renewable energy technologies.

2. Material and method

2.1. Description of CFD model

The CFD model used in this study is 2D, as its main focus is on the effect of double-pass geometry design on heat transfer. The upper and lower flow paths are compared to analyze the geometric differences. The PV panel is modeled as a thin cavity with a fixed temperature, given that this research focuses solely on the impact of variations in the upper and lower flow path geometries on heat transfer phenomena. The geometries studied are selected based on the upper-to-lower width size of 50 cm. Additionally, the distance between the outermost points of the geometric shape and the PV panel is kept constant to prevent continuity differences due to bends. Therefore, the analysis results will only be influenced by geometric characteristics. The shapes are shown in Fig. 1.

Fig. 1 illustrates the geometry variations, where four shapes are discussed in this study. Fig. 1(a) shows the comparison of the upper and lower paths in a 1:1 ratio; Fig. 1(b) shows the 1:4 upper and lower paths; Fig. 1(c) shows the 2:3 upper and lower paths; and finally, Fig. 1(d) shows the 3:2 upper and lower paths. These shapes are depicted below. In the CFD model, gravity is considered, air is treated as viscous and incompressible, and the walls are modeled as slip resistant. Thus, turbulent flow and heat convection occur between the walls and the flow.

The selection of the upper and lower channel geometry ratios was made to represent the general variation in channel shapes used in air-based PV/T systems. The 1:1 ratio in Fig. 1(a) represents the standard and symmetrical shape commonly used in previous studies, while Fig. 1(b) with a 1:4 ratio and Fig. 1(c) with a 2:3 ratio depict a narrower inlet flow distribution compared to the outlet cavity. Meanwhile, Fig. 1(d) with a 3:2 ratio represents a semi-compressed shape, where the flow in the upper cavity is wider than the outlet channel. Previous studies, such as those by [14] and [15], have shown that geometric shapes influence heat transfer performance in PV/T systems. This is further supported by Rajani et al., who demonstrated that variations in the channel depth ratio (D1/D2) can enhance the thermal efficiency of B-PVT systems by up to 8% through their influence on flow distribution and heat transfer [27]. Additionally, these shapes were selected because they can be practically applied to existing PV/T prototypes and as design considerations prior to the manufacturing process.

In the double-pass PV/T system, the fluid flow direction starts from the top, passing through a bend towards the bottom. By circulating the fluid through two paths, the double-pass system allows heat to be absorbed more efficiently by the solar panel, thereby improving the overall performance of the PV/T system. The flow direction scheme to be tested in the study, by examining each type of variation in the upper and lower flow paths, is shown in Fig. 2.

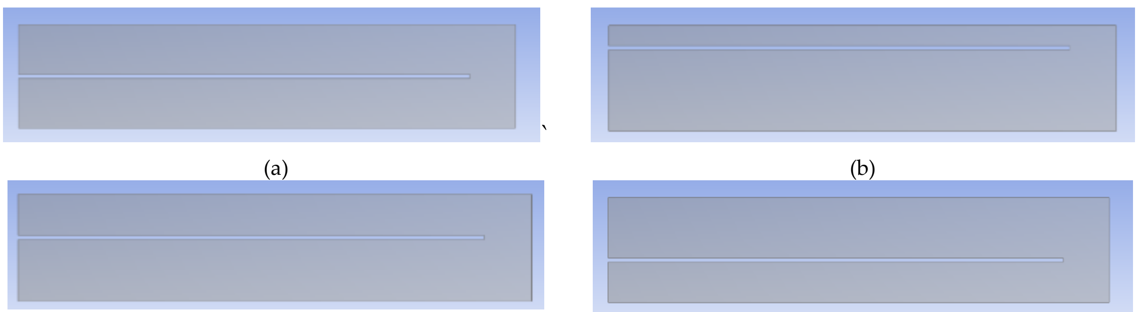

(a) (b) (c) (d)

Fig. 1. Illustration of cavity geometry variations (a) 1:1, (b) 1:4, (c) 2:3, and (d) 3:2.

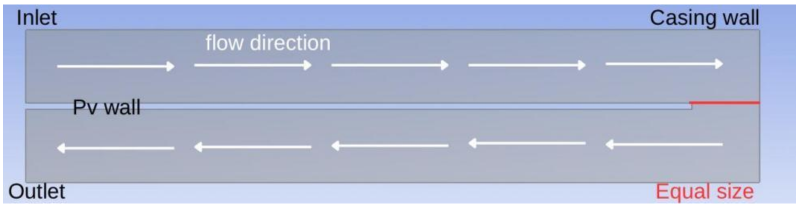

Fig. 2. Flow direction scheme of the PV/T system.

Table 1
Parameter B-PV/T

Parameter	Value
Length of B-PV	2.270 m
Box Length	2.500 m
PV and furthest return distance	0.23 m
Box width	0.52 m
PV width	0.02 m

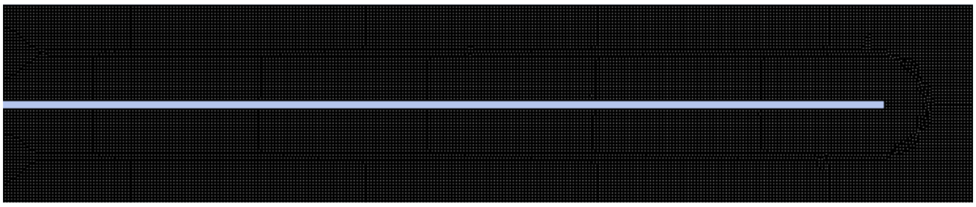

Fig. 3. Computational domain and grid.

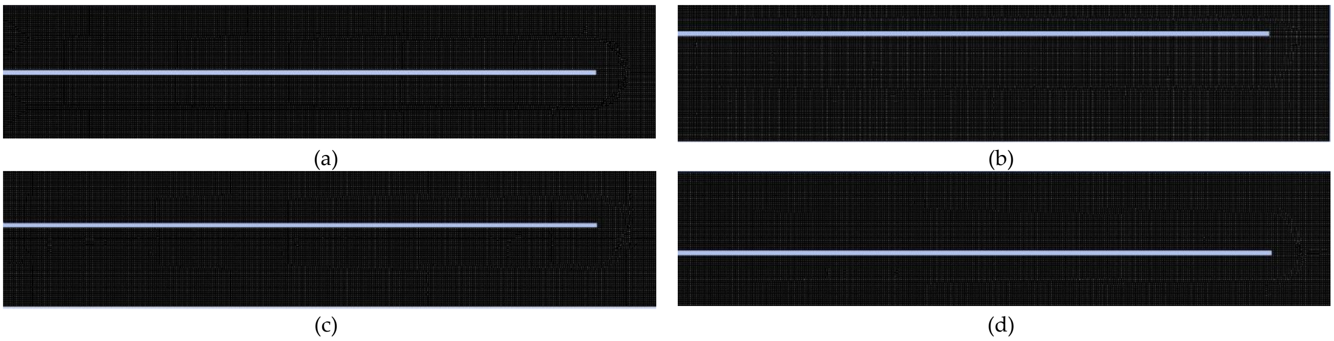

Fig. 4. Illustration of computational domain variations (a) 1:1, (b) 1:4, (c) 2:3, (d) 3:2.

The design size is based on the type of bifacial photovoltaic thermal (BPV) available in Indonesia. From the size of the BPV, it will be scaled down to the overall size of the B-PV/T system. The detailed domain specifications are shown in Table 1.

2.2. Computational domain and boundary conditions

The computational domain is discretized using the structured grid method. This will improve computational efficiency for the simulation. It will ensure lower residual results, implying more accurate computational outcomes. The structured grid is shown in Fig. 3. Fig. 3 shows the overall computational domain. These images were also created for each type of shape. Furthermore, Fig. 4 illustrates the case-by-case details that will be studied in this research. The figure explains the illustration of the computational domain variations: 1:1, 1:4, 2:3, and 3:2.

The boundary conditions used in this study are presented in Table 2. These conditions are designed to focus on the heat transfer process from the PV wall to the fluid flow. To achieve this, all walls except the PV wall are set to the same temperature as the inlet temperature. The PV wall temperature, set at 333.15 K (60°C) as a boundary condition, is based on experimental literature by Rajani et al. [29], which indicates that panel temperatures reach 60–70°C depending on radiation intensity, with bifacial PV (B-PV) recording values up to 75°C in tropical climates [27].

Table 2
Boundary conditions

Name	Momentum	Heat
Inlet	0.4 m/s < x>1.2 m/s	300 k
PV Wall	-	333.15 k
Casing Wall	-	300 k
Outlet	Calculated	Calculated

Thus, a temperature of 333.15 K is considered relevant and representative. The wall temperature of 300 K, equal to the inlet temperature, is set to focus the heat transfer analysis on the PV surface. This boundary condition aligns with Rajani et al. [15], who used a similar approach in research on u-turn shape geometry. Variations are applied only to the inlet velocity to analyze heat transfer behavior across different Reynolds numbers. The flow is assumed to be fully developed turbulent flow with a turbulence intensity of 10% at the inlet, a representative value for internal channel flow [30].

2.3. Governing equations

The numerical simulation of viscous flow with heat transfer in a two-dimensional (2D) airflow system is governed by the steady-state Navier-Stokes equations, comprising the continuity equation, momentum equation, and energy equation. These equations model turbulent fluid flow and heat transfer, considering only the x and y coordinate axes due to the 2D domain. Under steady-state conditions, temporal variations are neglected, and all variables are assumed constant over time, eliminating the need for transient terms in the governing equations.

The continuity equation ensures mass conservation and is expressed as:

$$\frac{\partial u}{\partial x} + v\frac{\partial v}{\partial y} = 0 \tag{1}$$

where u and v represent the velocity components in the x and y directions, respectively.

The momentum equation in the x-direction, accounting for viscous effects, pressure gradients, and buoyancy forces, is given by:

$$u\frac{\partial u}{\partial x} + v\frac{\partial u}{\partial y} = -\frac{1}{\rho}\frac{\partial p}{\partial x} + \mu\frac{\partial}{\partial x}\left(v\frac{\partial u}{\partial x}\right) + \frac{\partial}{\partial y}\left(v\frac{\partial u}{\partial y}\right) - g\beta f cos\alpha \tag{2}$$

where ρ is the fluid density, p is the pressure, v is the kinematic viscosity, g is the gravitational acceleration, β is the thermal expansion coefficient, and α is the angle of inclination.

The energy equation, describing heat transfer within the fluid, is formulated as:

$$u\frac{\partial T}{\partial x} + v\frac{\partial T}{\partial y} = \frac{\lambda_f}{\rho_f C_{pf}}\left[\frac{\partial^2 T}{\partial x^2} + \frac{\partial^2 T}{\partial y^2}\right] \tag{3}$$

where T is the temperature, λ_f is the thermal conductivity, ρ_f is the fluid density, and C_{pf} is the specific heat capacity at constant pressure.

The simulation's accuracy and convergence depend on several factors, including flow velocity, radiative heat transfer, and mesh size. Flow velocity influences the convective terms in the momentum and energy equations, affecting numerical stability. Radiative heat transfer, though not explicitly included in the energy equation, may be modeled through boundary conditions or additional source terms, impacting the temperature distribution. Mesh size determines the spatial resolution of the computational domain, with finer meshes enhancing accuracy but increasing computational cost. In this study, these factors are systematically analyzed to optimize the simulation's performance and ensure reliable results.

2.4. Validation

To validate the simulation in this study, a grid independence test was conducted to determine the ideal mesh [31]. This independence test is commonly performed in computational fluid dynamics (CFD) simulations to obtain optimal designs and achieve convergence [28].

Table 3
The grid independence test

Grid type	Grid size (mm)	Outlet temperature average (K)	Nodes	Skewness average	Orthogonal quality average
Very Coarse	10	310.214	13076	1.3779e-004	1
Coarse	7.5	310.145	45612	6.8638e-003	0.99971
Standard	5	309.845	51243	5.072e-004	1
Good	4	309.487	79734	3.2311e-003	0.99988
Very Good	3	309.406	141058	3.1076e-003	0.99989

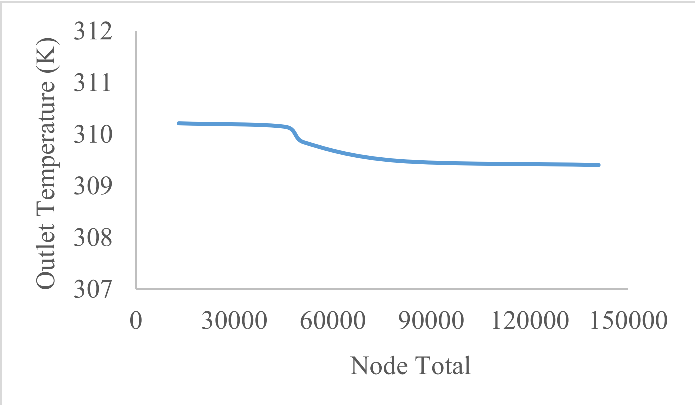

Fig. 5. Independence test result.

Fig. 6. Skewness and orthogonal quality [36].

This method was chosen and applied because no direct experimental data was available in this study and it is an important and proven aspect of performing CFD simulations without experimental validation, as was done in other studies [32], [33]. The grid independence test was performed by varying the grid size for the same geometry and comparing the results to ensure that the results were not affected by the grid size. The test was conducted using five different grid sizes, ranging from the coarsest at 10 mm to the finest at 3 mm [15], [34]. The flow velocity used in this test was 1.2 m/s, chosen because it is a commonly used value in the literature for air-based PV/T systems and provides stable simulation results. Although Fterich et al. [35] used a velocity of 2 m/s in their experiments, this study selected 1.2 m/s as it is more representative and numerically challenging for testing the influence of the grid on the outlet temperature. The results are shown in Table 3.

For a more intuitive illustration, the results and total number of grid nodes are shown graphically in Fig. 5. From the graph, it can be concluded that after 60,000 iterations of nodes, the output temperature does not show significant changes, indicating that it has reached a saturation point, as there are no significant differences in the results beyond that point. Therefore, in this study, all geometries use fine discretization with a grid size of 4 mm. This will ensure grid-independent values, thereby preventing excessive computational time costs.

Mesh quality is assessed based on the values of skewness and orthogonality. With a 4 mm grid, the skewness value is 0.0032311, indicating "excellent" quality, as shown in Fig. 6. The orthogonality value is 0.99988, also falling within the "excellent" range. An independence test is additionally performed to ensure the stability of the mesh quality control [36].

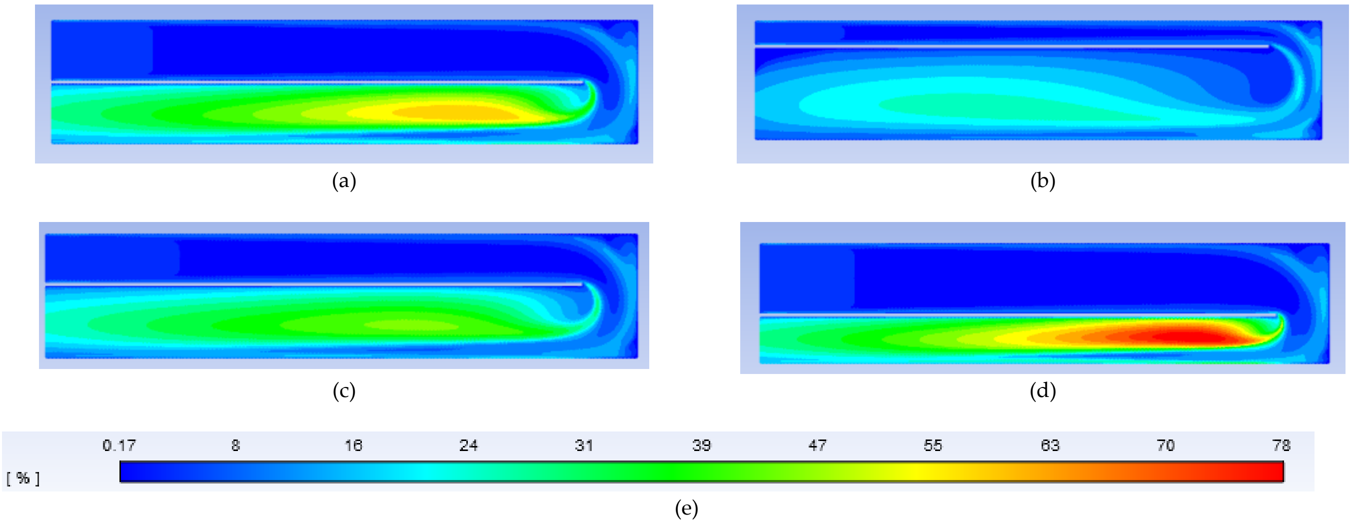

Fig. 7. Turbulence intensity contours (a) 1:1, (b) 1:4, (c) 2:3, (d) 3:2, and (e) Color legend for turbulence intensity.

2.5. CFD model selection

CFD model selection is an important step in numerical simulation to obtain accurate results and match the analyzed physical phenomena. In this research, the type of simulation carried out is steady state, because this approach considers conditions such as fluid flow velocity, temperature, and others in steady state to be compared with other variations. The turbulent model used is RANS (Reynolds-Averaged Navier-Stokes), which is commonly used in turbulent flow simulations due to its capabilities in various engineering applications. This model is effective in predicting turbulent flow characteristics in regions with high velocity gradients, such as those found in heat transfer applications. According to Wilcox [37], the k-ω SST (Shear Stress Transport) model excels in predicting turbulent flow near walls and turbulent transitions, especially in applications with high velocity gradients and fluid-structure interactions. The steady-state simulation is based on a study conducted by Patankar [38], explaining that steady simulation is more suitable for conditions where transient changes do not affect the results significantly. In addition, this simulation is more efficient in computational resources than a transient simulation. This approach is to evaluate the thermal and flow parameters in each configuration analyzed.

3. Results and discussion

This section presents the CFD simulation results for various cavity ratio configurations in the air-based PV/T system. The discussion focuses on three main parameters: turbulence intensity, effective thermal conductivity, and outlet air temperature. The impact of geometric modifications on thermal performance is critically analyzed and compared with relevant previous studies.

3.1. Turbulence intensity

To investigate the effects of the geometries studied in this research, the turbulence intensity distribution is analyzed. Turbulence intensity is closely related to heat transfer, where higher turbulence flow tends to enhance heat transfer efficiency. In the steady-state simulation, turbulence intensity is displayed for each geometry after reaching a steady condition. Fig. 7 shows the turbulence intensity distribution after the bend for each geometric shape tested. The data points used in the illustration were obtained with an inlet velocity of 1.2 m/s and a heat exposure of 1000 W/m². The selection of this high velocity helps highlight the differences in turbulence intensity distribution between the geometries, allowing for a clearer analysis of the impact of the shape.

Among these cases, the 3:2 configuration shows the largest area of high turbulence regions, as evidenced by the dominant red color near the bend of the cavity. Quantitatively, as shown in Figure 8, the maximum turbulence intensity reaches approximately 78% for the 3:2 configuration, significantly outperforming the 1:1 (57%), 2:3 (42.5%), and 1:4 (24.3%) ratios. The increased turbulence in the 3:2 configuration improves the convective heat transfer rate, as turbulent eddies promote better thermal mixing between the air and the PV panel surface. This observation is consistent with the research by Rajani et al. [15], which reported that configurations promoting higher turbulence can substantially enhance the thermal performance of PV/T systems. Parametric tests were also conducted to compare the performance of the shapes at different flow velocities. The comparison parameter is the maximum turbulence intensity.

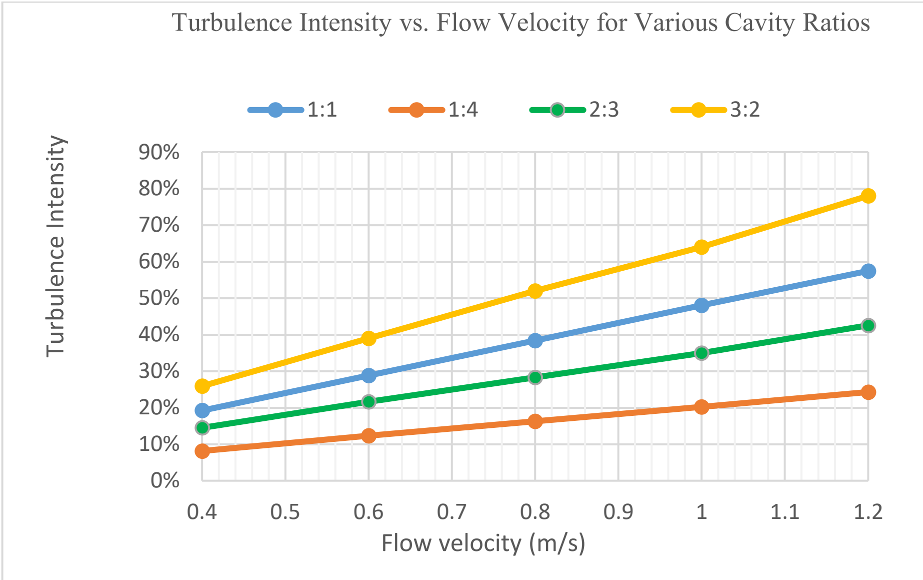

Fig. 8. Parametric analysis of turbulence intensity with turbulence intensity on the radius axis and flow velocity on the perimeter axis.

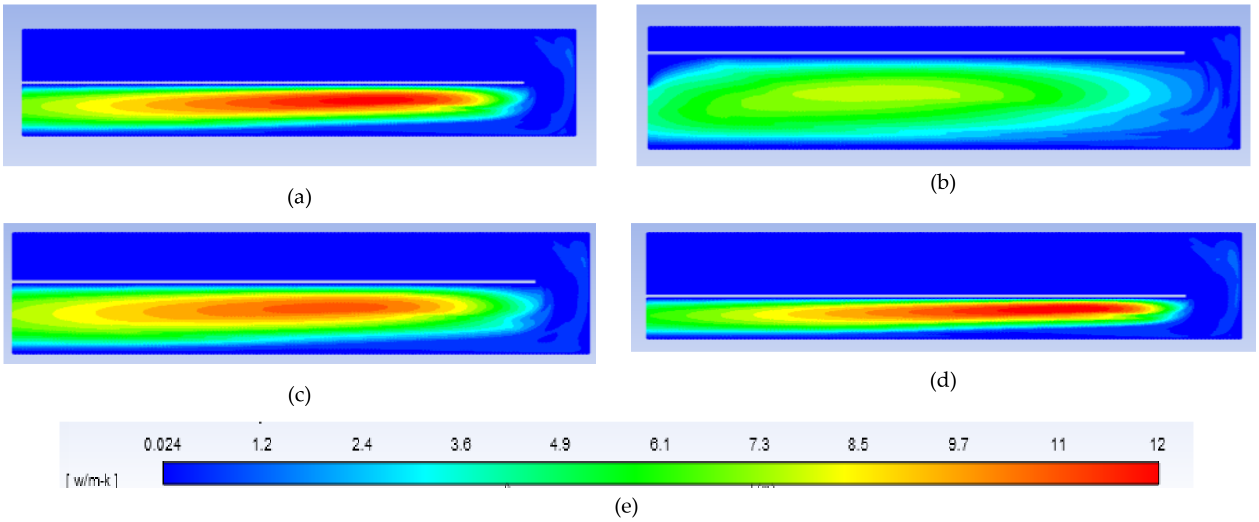

Fig. 9. Contours of effective thermal conductivity (a) 1:1, (b) 1:4, (c) 2:3, (d) 3:2, and (e) Color legend for effective thermal conductivity [W/m·K].

From Fig. 8, an increase in flow velocity results in an increase in turbulence intensity for all geometry shapes tested. As the flow velocity increases, each geometry shape shows a significant increase in turbulence values. In addition, the graph also shows that the 3:2 geometry excels in generating turbulence. The turbulence intensity at a flow velocity of 1.2 m/s reaches almost 78%, while for the other geometries the intensity is about 57% for 1:1, 42.55% for 2:3, and 24.29% for 1:4. This indicates that the 3:2 geometry can generate significantly more turbulence at higher flow velocities compared to the other geometries, causing greater flow disturbance. Meanwhile, the 1:4 geometry showed the lowest increase in turbulence of all the flow velocities tested. At a flow velocity of 1.2 m/s, its turbulence value remained at 24.29%, which is much lower compared to the 3:2 geometry or other geometries. This shows that the 1:4 geometry is more efficient in maintaining a steady flow with minimal turbulence, making it suitable for applications that require less flow disturbance.

3.2. Effective thermal conductivity

The next analysis focuses on effective thermal conductivity. The goal of this analysis is to understand how turbulence intensity affects heat transfer in the PV system. Theoretically, flows with higher turbulence levels can enhance the efficiency of heat transfer within the system. Fig. 9 presents the contours of effective thermal conductivity as a comparison for each bend shape variation. The data points used in this illustration are the same as those applied in the previous analysis.

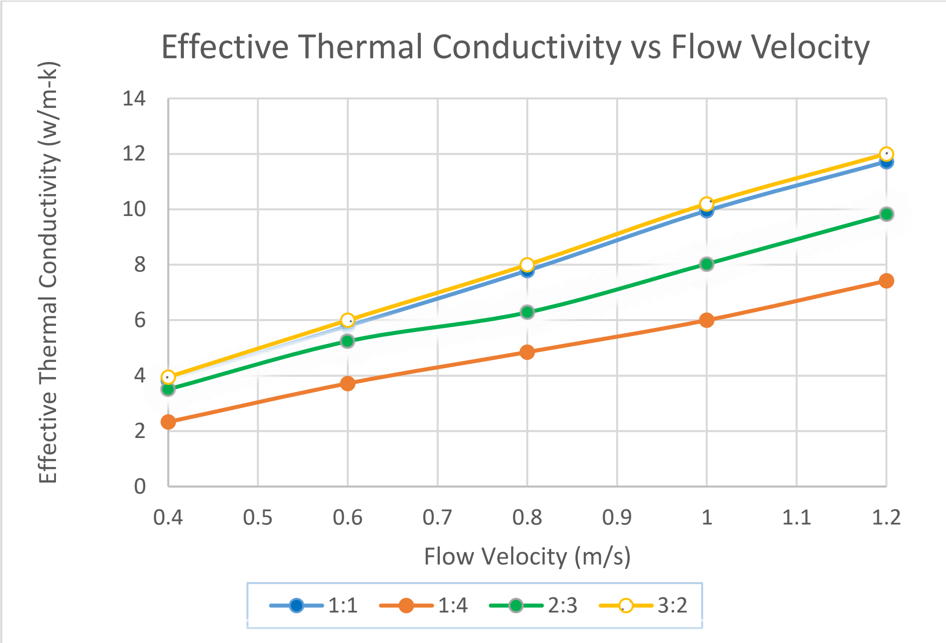

Fig. 10. Effective thermal conductivity versus flow velocity.

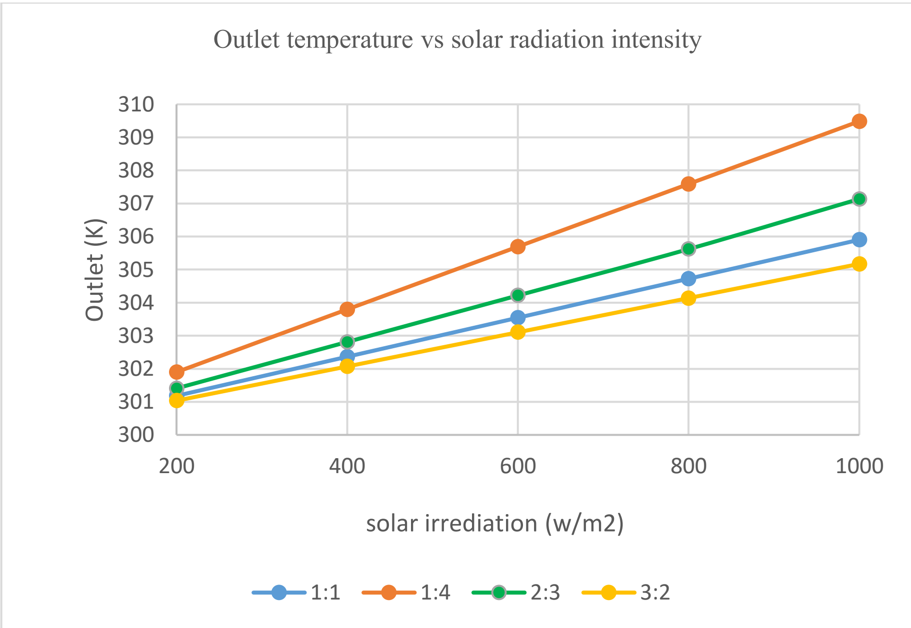

Fig. 11. Outlet temperature versus irradiation.

From the four images presented in Fig. 9, which show the contours of effective thermal conductivity, the distribution of thermal conductivity in various flow geometries can be observed. In Fig. 9(a), depicting the 1:1 geometry, the thermal conductivity distribution is relatively low, with most areas colored blue and green, indicating limited heat transfer efficiency. Fig. 9(b), showing the 1:4 geometry, shows a slight increase in thermal conductivity, with yellow and red areas indicating improved heat transfer efficiency in the central region, although overall it remains lower than the other geometries. In Fig. 9(c), depicting the 2:3 geometry, the thermal conductivity distribution is higher, with more areas colored yellow and red, indicating that this geometry is more efficient in facilitating heat transfer, thanks to increased turbulence and fluid mixing. Finally, Fig. 9(d) depicting the 3:2 geometry shows the highest thermal conductivity, especially in the red areas, indicating very good heat transfer efficiency, most likely due to increased turbulence that enhances fluid mixing.

Similar results can be observed in Fig. 10, which shows the relationship between flow velocity and effective thermal conductivity for each geometry. The 1:1 geometry (blue line) shows the slowest increase in thermal conductivity as flow velocity increases. The 1:4 geometry (orange line) has a sharper increase but remains at a lower level compared to the 2:3 (green line) and 3:2 (yellow) geometries. The 3:2 geometry shows the most significant increase in thermal conductivity, further highlighting the effectiveness of this geometry in enhancing heat transfer as flow velocity increases. These findings are consistent with the study by Prasetyo et al. [14], which emphasizes that more intense turbulence plays a crucial role in maximizing thermal energy extraction.

3.3. Outlet temperature

Many air-based PV/T systems are used for drying, where the hot air generated by the system flows into the drying chamber. For such systems, a high outlet air temperature is required. For this reason, this section will focus on outlet air temperature. Turbulence intensity and effective thermal conductivity must contribute to increasing the flow temperature. In the context of BPV-T, the higher the outlet temperature, the more effective the drying and cooling of the PV module, which prevents the PV from overheating and maintains its efficiency. The process of heating the outlet temperature is illustrated by plotting the outlet temperature against solar radiation intensity, as shown below. The data points used for this comparison are based on a flow velocity of 1.2 m/s, and each wall and PV wall parameter is set at a temperature of 300 K, making it easier to observe the differences between the various configurations.

Fig. 11 shows the relationship between solar heat flux (W/m²) and outlet air temperature (K) for four cavity configurations: 1:1, 1:4, 2:3, and 3:2. The 1:4 configuration (orange line) consistently achieves the highest outlet temperatures across all tested heat flux levels, indicating superior heat capture performance. In contrast, the 1:1 (blue line) and 2:3 (green line) configurations show moderate outlet temperatures, suggesting a balance between thermal regulation and heat extraction. The 3:2 configuration (yellow), although demonstrating superior turbulence and effective thermal conductivity in previous analyses, shows lower outlet temperatures compared to the 1:4 configuration, indicating that its heat transfer enhancement focuses more on distribution efficiency rather than temperature increase.

Based on the parametric analysis of outlet temperature and perimeter axis flow velocity in Fig. 12, the 3:2 geometry, which excels in turbulent intensity parameters and effective thermal conductivity, shows the lowest temperature increase among others. As for the 1:4 geometry, which previously had the lowest turbulent intensity and effective thermal conductivity, it got the highest temperature increase among other geometries. This investigation is in line with the findings of previous research conducted by Vlahostegios et al. [39] explaining that an increase in turbulent intensity will also increase convective heat transfer with rapid flow mixing. This makes the outlet temperature lower due to more uniform heat distribution. In this case, although the 3:2 geometry optimizes the overall heat distribution and energy absorption, making it have a low outlet temperature, it is different from the 1:4 geometry case, which can produce the highest outlet temperature. Therefore, it is felt that this geometry can be utilized for drying applications that require high air temperatures.

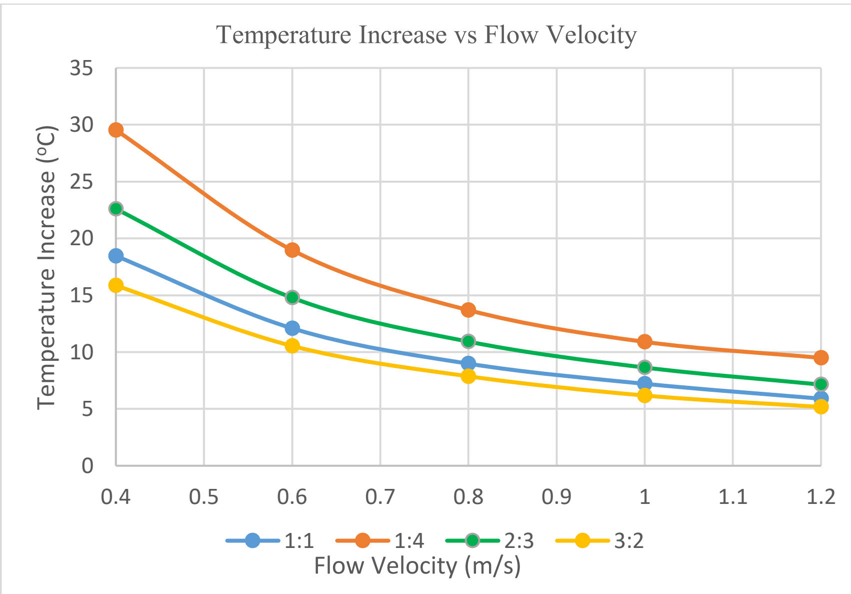

Fig. 12. Temperature increase (°C) versus flow velocity.

4. Conclusions

This study examines how heat transfer performance and thermal properties are affected by various upper-to-lower cavity ratio adjustments in air-based photovoltaic thermal (PV/T) systems with a double-pass flow path. To do this, turbulence intensity, effective thermal conductivity, and outlet temperature in a variety of cavities with ratios of 1:1, 1:4, 2:3, and 3:2 were examined using Computational Fluid Dynamics (CFD) simulations. The results show that the 3:2 arrangement has the best effective thermal conductivity and regularly produces the maximum turbulence intensity, around 78%. This implies that the arrangement maximizes flow, which raises the effectiveness of heat transfer. On the other hand, the 1:4 configuration produces the highest output temperature of 29°C of any variation, making it a better option for applications like PV/T-based drying systems that place a higher priority on outlet temperature.

These results underscore the necessity of a customized approach to cavity ratio selection in air-based PV/T design, contingent on the unique requirements of each application. The 3:2 configuration has been identified as a promising solution for various applications, including active cooling systems for PV modules, thermal energy storage, and solar-powered room heating. In these contexts, high heat transfer efficiency is a critical factor. Conversely, the 1:4 configuration is more suitable for agricultural drying systems, hot air desalination, or industrial processes that necessitate high-temperature air due to its capacity to generate higher outlet temperatures.

Based on this, it can be concluded that the choice of upper and lower cavity variations in bifacial PV/T significantly reduces the thermal efficiency of PV/T. In addition, this study highlights the importance of geometry adjustment in the PV/T design optimization process to comprehensively improve the site and heat transfer performance.

Declaration statement

Nabil Putra Wahyu Yanuariska: Collecting data, Methodology, and Writing-Original Draft. **Nia Nuraeni Suryaman:** Conceptualization, Supervision. **Ahmad Rajani**: Writing Review and Editing.

Acknowledgement

The authors would like to thank Widyatama University, Bandung, Indonesia and the National Research and Innovation Agency (BRIN), Bandung, Indonesia for facilitating all data collection and providing complete literature in the completion of this work. Thanks are also extended to all Widyatama lecturers, BRIN researchers, staff, and research assistants who have assisted in the completion of this research.

Disclosure statement

The author declares that this manuscript is free from conflict of interest and is processed by applicable journal provisions and policies to avoid deviations from publication ethics in various forms.

Funding statement

The authors received no funding for this research.

Data availability statement

The authors confirm that the data supporting the findings of this study are available within the article or its supplementary materials.

AI Usage Statement

Generative AI and AI-assisted tools were used to enhance the language and readability of this manuscript. The authors have reviewed and revised all AI-generated content to ensure its accuracy and alignment with the research. The authors remain fully responsible for the work's scientific content, conclusions, and integrity, and disclose the use of AI to ensure transparency and adherence to publisher guidelines.

References

[1] H. H. Pourasl, R. V. Barenji, and V. M. Khojastehnezhad, "Solar energy status in the world: A comprehensive review," *Energy Reports*, vol. 10, pp. 3474–3493, Nov. 2023, doi: 10.1016/j.egyr.2023.10.022.

[2] A. Kharisma, S. Pinandita, and A. E. Jayanti, "Literature review: Kajian potensi energi surya alternatif energi listrik," *Jurnal Energi Baru dan Terbarukan*, vol. 5, no. 2, pp. 145–154, Jul. 2024, doi: 10.14710/jebt.2024.23956.

[3] A. S. Pramudiyanto and S. W. A. Suedy, "Energi bersih dan ramah lingkungan dari biomassa untuk mengurangi efek gas rumah kaca dan perubahan iklim yang ekstrim," *Jurnal Energi Baru dan Terbarukan*, vol. 1, no. 3, pp. 86–99, Oct. 2020, doi: 10.14710/jebt.2020.9990.

[4] A. O. M. Maka and J. M. Alabid, "Solar energy technology and its roles in sustainable development," *Clean Energy*, vol. 6, no. 3, pp. 476–483, Jun. 2022, doi: 10.1093/ce/zkac023.

[5] D. Wen, W. Gao, F. Qian, Q. Gu, and J. Ren, "Development of solar photovoltaic industry and market in China, Germany, Japan and the United States of America using incentive policies," *Energy Exploration & Exploitation*, vol. 39, no. 5, pp. 1429–1456, Sep. 2021, doi: 10.1177/0144598720979256.

[6] S. Comello, S. Reichelstein, and A. Sahoo, "The road ahead for solar PV power," *Renewable and Sustainable Energy Reviews*, vol. 92, pp. 744–756, Sep. 2018, doi: 10.1016/j.rser.2018.04.098.

[7] K. Basyar, Z. Arifin, D. D. D. P. Tjahjana, and S. D. Prasetyo, "Analysis of the impact of different fin configurations as passive coolants on photovoltaic performance," *International Journal of Heat and Technology*, vol. 42, no. 6, pp. 2115–2124, Dec. 2024, doi: 10.18280/ijht.420630.

[8] S. Zine, B. Djedjiga, S. Fethya, L. Salah, and B. Ahmed, "Experimental study of hybrid photovoltaic (PV/T) thermal solar collector with air cooling for domestic use: A thermal and electrical performances evaluation," *Journal of Advanced Research in Fluid Mechanics and Thermal Sciences*, vol. 116, no. 1, pp. 170–183, Apr. 2024, doi: 10.37934/arfmts.116.1.170183.

[9] K. S. Kramer, S. Mehnert, G. Munz, S. Helmling, and M. Lämmle, "Photovoltaic thermal technology collectors, systems, and applications," *Energy Technology*, vol. 11, no. 12, Dec. 2023, doi: 10.1002/ente.202300378.

[10] A. Chauhan, V. V. Tyagi, and S. Anand, "Futuristic approach for thermal management in solar PV/thermal systems with possible applications," *Energy Conversion and Management*, vol. 163, pp. 314–354, May 2018, doi: 10.1016/j.enconman.2018.02.008.

[11] J.-H. Kim, S.-M. Kim, and J.-T. Kim, "Experimental performance of an advanced air-type photovoltaic/thermal (PVT) collector with direct expansion air handling unit (AHU)," *Sustainability*, vol. 13, no. 2, p. 888, Jan. 2021, doi: 10.3390/su13020888.

[12] M. Patil, A. Sidramappa, A. M. Hebbale, and J. S. Vishwanatha, "Computational fluid dynamics (CFD) analysis of air-cooled solar photovoltaic (PV/T) panels," *Materials Today: Proceedings*, vol. 100, pp. 93–101, 2024, doi: 10.1016/j.matpr.2023.05.198.

[13] X. Yang, L. Sun, Y. Yuan, X. Zhao, and X. Cao, "Experimental investigation on performance comparison of PV/T-PCM system and PV/T system," *Renewable Energy*, vol. 119, pp. 152–159, Apr. 2018, doi: 10.1016/j.renene.2017.11.094.

[14] S. D. Prasetyo *et al.*, "Optimization of photovoltaic thermal collectors using fins: A review of strategies for enhanced solar energy harvesting," *Mathematical Modelling of Engineering Problems*, vol. 10, no. 4, pp. 1235–1248, Aug. 2023, doi: 10.18280/mmep.100416.

[15] A. Rajani *et al.*, "U-turn shape effect on effective thermal conductivity of double pass photovoltaic thermal (PVT) systems configuration," *CFD Letters*, vol. 17, no. 5, pp. 12–25, Nov. 2024, doi: 10.37934/cfdl.17.5.1225.

[16] S.-B. Kim, K.-A. Moon, B.-H. An, K.-H. Choi, and H.-U. Choi, "Experimental performance evaluation of air-based photovoltaic–thermal collector with rectangular turbulators and longitudinal fins," *Energy Reports*, vol. 12, pp. 1315–1324, Dec. 2024, doi: 10.1016/j.egyr.2024.07.038.

[17] Amrizal, Y. P. Hidayat, and M. Irsyad, "Performance comparison of single and double pass PV/T solar collectors integrated with rectangular plate fin absorber," in *IOP Conference Series: Materials Science and Engineering*, vol. 1173, no. 1, p. 012023, Aug. 2021, doi: 10.1088/1757-899X/1173/1/012023.

[18] H. A. Kazem, "Evaluation and analysis of water-based photovoltaic/thermal (PV/T) system," *Case Studies in Thermal Engineering*, vol. 13, p. 100401, Mar. 2019, doi: 10.1016/j.csite.2019.100401.

[19] A. L. Abdullah, S. Misha, N. Tamaldin, M. A. M. Rosli, and F. A. Sachit, "Theoretical study and indoor experimental validation of performance of the new photovoltaic thermal solar collector (PVT) based water system," *Case Studies in Thermal Engineering*, vol. 18, p. 100595, Apr. 2020, doi: 10.1016/j.csite.2020.100595.

[20] G. Barone, A. Buonomano, C. Forzano, A. Palombo, and O. Panagopoulos, "Photovoltaic thermal collectors: Experimental analysis and simulation model of an innovative low-cost water-based prototype," *Energy*, vol. 179, pp. 502–516, Jul. 2019, doi: 10.1016/j.energy.2019.04.140.

[21] G. Badran and M. Dhimish, "A comparative study of bifacial versus monofacial PV systems at the UK's largest solar plant," *Clean Energy*, vol. 8, no. 4, pp. 248–260, Aug. 2024, doi: 10.1093/ce/zkae043.

[22] J. Jang and K. Lee, "Practical performance analysis of a bifacial PV module and system," *Energies*, vol. 13, no. 17, p. 4389, Aug. 2020, doi: 10.3390/en13174389.

[23] W. Gu, T. Ma, S. Ahmed, Y. Zhang, and J. Peng, "A comprehensive review and outlook of bifacial photovoltaic (bPV) technology," *Energy Conversion and Management*, vol. 223, p. 113283, Nov. 2020, doi: 10.1016/j.enconman.2020.113283.

[24] D. Kurz *et al.*, "An analysis of the increase in energy efficiency of photovoltaic installations by using bifacial modules," *Energies*, vol. 18, no. 5, p. 1296, Mar. 2025, doi: 10.3390/en18051296.

[25] A. Gagliano, G. M. Tina, S. Aneli, and S. Nižetić, "Comparative assessments of the performances of PV/T and conventional solar plants," *Journal of Cleaner Production*, vol. 219, pp. 304–315, May 2019, doi: 10.1016/j.jclepro.2019.02.038.

[26] W. E. Ewe, K. Sopian, M. Mohanraj, A. Fudholi, N. Asim, and A. Ibrahim, "Exergetic performance of jet impingement bifacial photovoltaic-thermal solar air collector with different packing factors and jet distributions," *Heat Transfer Engineering*, vol. 45, no. 10, pp. 904–914, May 2024, doi: 10.1080/01457632.2023.2227807.

[27] A. Rajani *et al.*, "Multi-objective optimisation and sensitivity analysis of component influences on efficiency in air-based bifacial photovoltaic thermal systems (B-PVT)," *International Journal of Renewable Energy Development*, vol. 13, no. 4, pp. 736–749, Jul. 2024, doi: 10.61435/ijred.2024.60212.

[28] W. M. Shaban, A. E. Kabeel, M. El Hadi Attia, and F. M. Talaat, "Optimizing photovoltaic thermal solar systems efficiency through advanced artificial intelligence driven thermal management techniques," *Applied Thermal Engineering*, vol. 247, p. 123029, Jun. 2024, doi: 10.1016/j.applthermaleng.2024.123029.

[29] V.-S. Hudișteanu, N.-C. Chereches, F.-E. Țurcanu, I. Hudișteanu, and C. Romila, "Impact of temperature on the efficiency of monocrystalline and polycrystalline photovoltaic panels: A comprehensive experimental analysis for sustainable energy solutions," *Sustainability*, vol. 16, no. 23, p. 10566, Dec. 2024, doi: 10.3390/su162310566.

[30] S. B. Pope, *Turbulent Flows*. Cambridge, UK: Cambridge University Press, 2000, doi: 10.1017/CBO9780511840531.

[31] M. A. Talib, A. A. Eidan, A. H. Tawfeeq, and F. M. K. AL-Fatlawe, "Effect of changing the water flow rate on the efficiency of hybrid PV/T uncovered collectors without glasses: Numerical study," *CFD Letters*, vol. 16, no. 2, pp. 91–104, Nov. 2023, doi: 10.37934/cfdl.16.2.91104.

[32] S. Kasmaiee, S. Kasmaiee, and A. Farshad, "Unsteady CFD simulation of a rotor blade under various wind conditions," *Scientific Reports*, vol. 14, no. 1, p. 19176, Aug. 2024, doi: 10.1038/s41598-024-70350-5.

[33] A. Wodołażski, N. Howaniec, B. Jura, A. Bąk, and A. Smoliński, "CFD numerical modelling of a PV–TEG hybrid system cooled by air heat sink coupled with a single-phase inverter," *Materials*, vol. 14, no. 19, p. 5800, Oct. 2021, doi: 10.3390/ma14195800.

[34] E. Gül, Z. Kılıç, E. İkincioğulları, and M. C. Aydın, "Investigation of the effect of variable-sized energy dissipating blocks on sluice gate performance," *Water SA*, vol. 50, no. 1, pp. 1–10, Jan. 2024, doi: 10.17159/wsa/2024.v50.i1.4064.

[35] M. Fterich, H. Chouikhi, S. Sandoval-Torres, H. Bentaher, A. Elloumi, and A. Maalej, "Numerical simulation and experimental characterization of the heat transfer in a PV/T air collector prototype," *Case Studies in Thermal Engineering*, vol. 27, p. 101209, Oct. 2021, doi: 10.1016/j.csite.2021.101209.

[36] N. Fatchurrohman and S. T. Chia, "Performance of hybrid nano-micro reinforced mg metal matrix composites brake calliper: Simulation approach," in *IOP Conference Series: Materials Science and Engineering*, vol. 257, p. 012060, Oct. 2017, doi: 10.1088/1757-899X/257/1/012060.

[37] D. C. Wilcox, *Turbulence Modeling for CFD*, 2nd ed. La Cañada, CA: DCW Industries, 1998.

[38] S. V. Patankar, *Numerical Heat Transfer and Fluid Flow*. Boca Raton, FL: CRC Press, 2018, doi: 10.1201/9781482234213.

[39] Z. Vlahostergios, D. Missirlis, M. Flouros, C. Albanakis, and K. Yakinthos, "Effect of turbulence intensity on the pressure drop and heat transfer in a staggered tube bundle heat exchanger," *Experimental Thermal and Fluid Science*, vol. 60, pp. 75–82, Jan. 2015, doi: 10.1016/j.expthermflusci.2014.08.011.

Authors information

Nabil Putra Wahyu Yanuariska is a student of Mechanical Engineering Department, Widyatama University, Bandung, Indonesia. He is active in research and community service as well as other non-academic activities. His areas of interest are Energy Conversion, simulation, social project and Renewable Energy.

Nia Nuraeni Suryaman is a lecturer at Widyatama University Mechanical Engineering Study Program. Master of Mechanical Engineering, Pasundan University Bandung. Research on energy, renewable energy, temperature distribution, RHVAC.

Ahmad Rajani has been a researcher since 2015 and is currently a member of the RC for Energy Conversion and Conservation at the National Research and Innovation Agency (BRIN). He graduated with a B.S. in Electrical Engineering in 2004, an M.T. in Electrical Engineering in 2012, and is now a PhD student in Electrical Engineering at University Technology Malaysia (UTM). His research focuses on photovoltaics, solar energy engineering, and renewable energy technology. He is currently concentrating on photovoltaic thermal (PVT) systems, with a particular emphasis on bifacial photovoltaic modules and the optimization of renewable energy systems through advanced modeling and simulation techniques. Mr. Rajani has published several peer-reviewed papers, including articles indexed in Scopus and the Web of Science, reflecting his extensive contributions to the field. He also holds several patents related to renewable energy technologies. In addition to his research activities, he has actively participated in community service projects aimed at promoting sustainable energy solutions. He can be contacted via email at ahmad.rajani@brin.go.id.